ARTICLE

ACS chemical biology

Indo-1 Derivatives for Local Calcium Sensing

Michael Bannwarth[†,¶], Ivan R. Corrêa, Jr.[†,¶], Monika Sztretye[‡], Sandrine Pouvreau[‡,§], Cindy Fellay[†], Annina Aebischer[†], Leandro Royer[‡], Eduardo Ríos[‡,*], and Kai Johnsson[†,*]

[†]Institute of Chemical Sciences and Engineering, École Polytechnique Fédérale de Lausanne (EPFL), CH-1015, Lausanne, Switzerland and [‡]Section of Cellular Signaling, Department of Molecular Biophysics and Physiology, Rush University, 1750 West Harrison Street, Suite 1279JS, Chicago, Illinois 60612. [¶]These authors contributed equally to this work. [§]Present address: Physiologie Intégrative Cellulaire et Moléculaire, Université Claude Bernard Lyon 1, Villeurbanne Cedex, France

ABSTRACT The role of calcium in signal transduction relies on the precise spatial and temporal control of its concentration. The existing means to detect fluctuations in Ca^{2+} concentrations with adequate temporal and spatial resolution are limited. We introduce here a method to measure Ca^{2+} concentrations in defined locations in living cells that is based on linking the Ca^{2+}-sensitive dye Indo-1 to SNAP-tag fusion proteins. Fluorescence spectroscopy of SNAP-Indo-1 conjugates *in vitro* showed that the conjugates retained the Ca^{2+}-sensing ability of Indo-1. In a proof-of-principle experiment, local Ca^{2+} sensing was demonstrated in single cells dissociated from muscle of adult mice expressing a nucleus-localized SNAP-tag fusion. Ca^{2+} concentrations inside nuclei of resting cells were measured by shifted excitation and emission ratioing of confocal microscopic images of fluorescence. After permeabilizing the plasma membrane, changes in the bathing solution induced corresponding changes in nuclear [Ca^{2+}] that were readily detected and used for a preliminary calibration of the technique. This work thus demonstrates the synthesis and application of SNAP-tag-based Ca^{2+} indicators that combine the spatial specificity of genetically encoded calcium indicators with the advantageous spectroscopic properties of synthetic indicators.

The calcium ion is a ubiquitous messenger that plays multiple crucial roles in intra- and intercellular signaling (*1*). To separate the multiplicity of signals conveyed by this messenger, some of them must be encoded in elaborate spatial and temporal patterns. The spatial localization takes the form of small domains of elevated concentration, established usually for brief periods near the mouth of calcium channels that connect the cytosol to Ca^{2+}-rich compartments such as the endoplasmic reticulum (ER) or the extracellular space. For example, calcium is passed from the ER to mitochondria near inositol triphosphate receptor channels, even though there is no actual pore connecting the lumen of these organelles (*2*). A number of local calcium signaling events have been observed in cells and assigned various names, including sparks, embers, puffs, and blips (*3*).

The two main approaches currently used for the visualization of calcium signaling in cells are based either on genetically encoded fluorescent Ca^{2+} indicator proteins (FCIPs) or on synthetic fluorescent Ca^{2+} indicators. FCIPs are designed to bind Ca^{2+} in a way that either leads to changes in fluorescence resonance energy transfer between two different fluorescent proteins that are part of the indicator protein (*4, 5*) or modifies the properties of a single fluorescent protein (*6, 7*). The most attractive feature of FCIPs is the possibility of targeted expressions, for example, in tissues, cell types, or organelles and subcellular locations (*8*). However, despite continuous improvements of the various FCIPs (*9, 10*), these indicators still suffer from a number of drawbacks. The response of the available FCIPs typically has a low dynamic range (*DR*, defined as the ratio of signals of the free and Ca^{2+}-bound dye; for ratiometric indicators R_{max}/R_{min}) and is slow in comparison to physiological calcium signals. Furthermore, the interaction with other cel-

***Corresponding authors:**
erios@rush.edu,
kai.johnsson@epfl.ch.

Received for review October 21, 2008 and accepted January 30, 2009.

Published online February 4, 2009

10.1021/cb800258g CCC: $40.75

lular proteins can affect their performance (*8*), and the size of FCIPs can be rather large, 650 amino acids for cameleons (*4*).

An alternative for the visualization of local calcium signals is the use of small synthetic fluorescent indicators modified for localization to specific sites within the cell. Positively charged indicators such as rhod-2 tend to accumulate in the mitochondrial matrix (*11*). Indicator dextran conjugates remain in the cytoplasm; Calcium Green dextran modified with a nuclear localization sequence peptide has been used to measure $[Ca^{2+}]$ in the nucleus (*12*) and indicator stearyl ($C_{18}H_{37}$) derivatives were used to place a Ca^{2+} monitor near membranes (*13*). More advanced techniques rely on small synthetic indicators and/or localized proteins of interest that form a "hybrid indicator" in cells. One approach for localizing calcium indicators in cells is based on the use of fusion proteins displaying peptides with high affinity for Texas red and X-rhod; however, this approach has not yet been used for monitoring $[Ca^{2+}]$ in cells (*14*). More recently, a biarsenical derivative of Calcium Green has been synthesized that specifically labels fusion proteins possessing a tetracysteine tag (*15*). The approach has been used to report rapid $[Ca^{2+}]$ dynamics at gap junctions, thereby demonstrating the enormous potential of hybrid indicators. However, the tetracysteine tag cannot be easily used in the lumen of the endoplasmic or sarcoplasmic reticulum because of disulfide bond formation, and no ratiometric Ca^{2+} indicators for labeling of the tetracysteine tag are available.

Indo-1 is a very useful synthetic Ca^{2+} indicator for flow cytometry and confocal microscopy, as its excitation using one of the argon laser lines yields an emission spectrum that depends on $[Ca^{2+}]$ and therefore can be used for ratiometric measurements (*16*). Furthermore, the excitation spectra of Indo-1 and its low-affinity relative Mag-Indo-1 are also shifted upon binding Ca^{2+}, a feature exploited in the SEER (shifted excitation and emission ratioing) technique (*17*) to greatly increase its Ca^{2+} sensitivity. Indo-1 is a rapidly responding Ca^{2+} indicator, although its kinetics can be altered under cellular conditions (*18*). The dye has been coupled to microspheres for long-time Ca^{2+} sensing inside living cells after endocytosis of the microspheres, but the precise localization of the microspheres was not determined (*19*). Coupling the indicator to microspheres or dextran prevents Indo-1 not only from leaking out of cells but also from rapid diffusion and can therefore be helpful for local calcium concentration measurements (*20*). However, the coupling of Indo-1 to a localized protein inside cells has not been achieved so far.

Here we report the specific localization of Indo-1 in cells *via* the SNAP-tag fusion protein technology. Derivatives of Indo-1 linked to benzylguanine, the substrate of SNAP-tag, were synthesized and used for the labeling of SNAP-tag fusion proteins. Indo-1-labeled SNAP-tag fusion proteins were characterized as Ca^{2+} reporters *in vitro*, and it was shown that the labeled fusion proteins can be used to measure $[Ca^{2+}]$ changes in the 50 nM to 2 μM range. Finally, the Indo-1 derivatives were used for measuring nuclear $[Ca^{2+}]$ ($[Ca^{2+}]_n$) in resting cultured primary muscle cells of an adult mouse expressing nuclear localized SNAP-tag.

RESULTS AND DISCUSSION

SNAP-tag (182 amino acids) is an engineered human O^6-alkylguanine-DNA alkyltransferase (AGT) that specifically reacts with O^6-benzylguanine (BG) derivatives (*21, 22*). SNAP-tag fusion proteins can be labeled with a large variety of spectroscopic probes inside living cells with no restrictions with respect to organelles or localization (*23*). The synthesis of BG-Indo-1 derivatives should therefore permit the measurement of $[Ca^{2+}]$ with both high spatial and temporal resolution in living cells (Figure 1).

Below, we first describe the synthesis of the BG-Indo-1 derivatives and characterize their spectral properties before and after reaction with SNAP-tag fusion proteins. Then we demonstrate the ability of the new Indo-1 derivatives to label SNAP-tag fusions in cultured primary muscle cells of mice and to respond to changes in $[Ca^{2+}]_n$.

Synthesis of Indo-1 Derivatives. To couple BG to Indo-1, we chose the indole carboxyl group (Figure 1, panel b), which was previously used for the coupling of Indo-1 to microspheres (*19*). Our synthesis started from the previously described Indo-1 ethyl ester **1** (Scheme 1), which was prepared in eight steps from *o*-nitrophenol (Supporting Information). Compound **1** was coupled to benzylguanine amine (BG-NH_2, **2**) and to a BG amine derivative containing a polyethylene glycol linker (BG-PEG_4-NH_2, **5**) in order to study the influence of the linker length on the spectroscopic properties of the indicator. Subsequent alkaline hydrolysis of the ethyl esters yielded the Indo-1 derivatives BG1-Indo-1 and BG2-Indo-1.

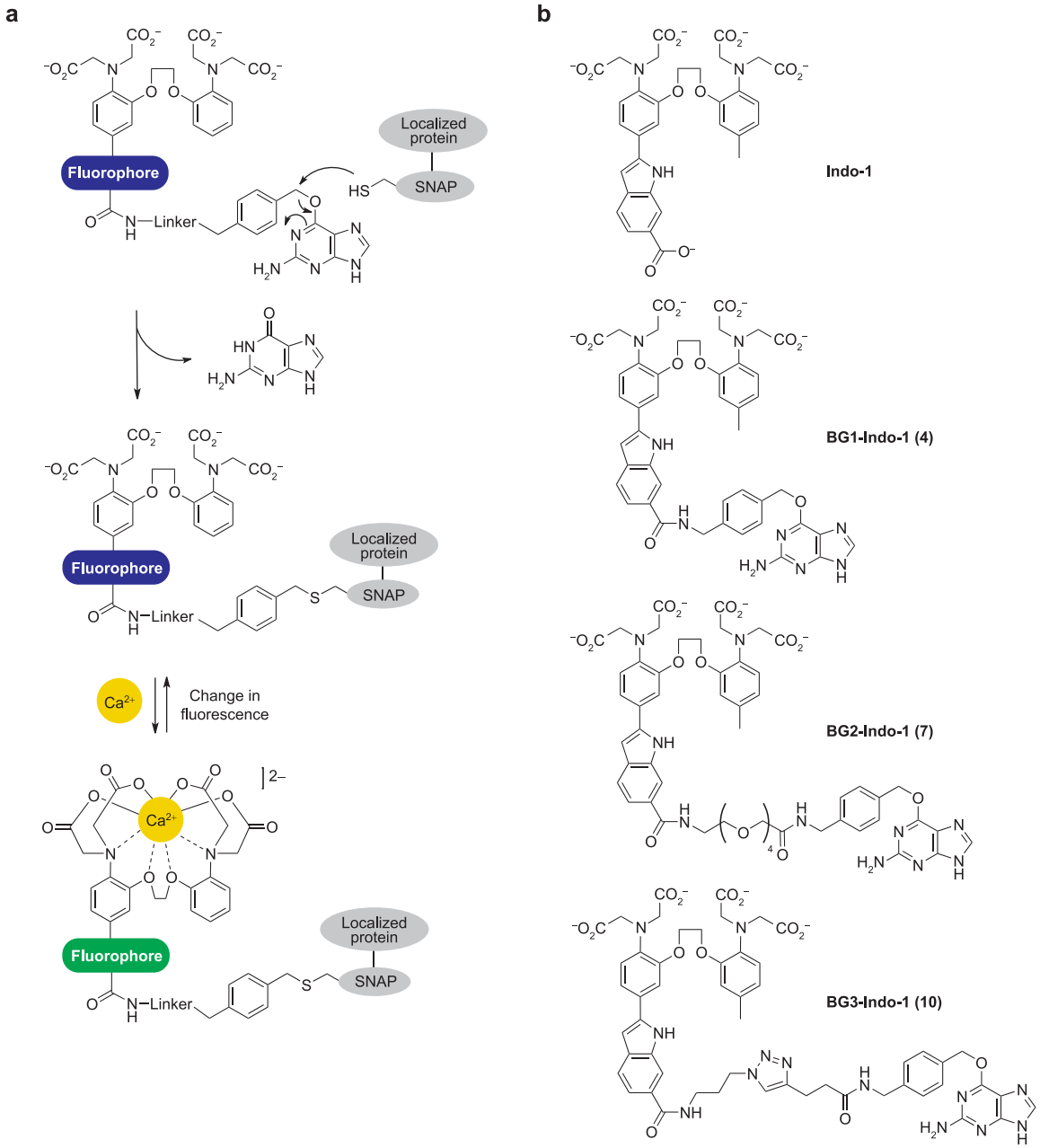

Figure 1. Use of SNAP-tag technology for the localization of Indo-1 in living cells. a) Mechanism for localizing Ca^{2+} indicators in cells *via* SNAP-tag fusion proteins. b) Structure of Indo-1 and Indo-1 benzylguanine (BG) derivatives synthesized in this work.

Negatively charged tetracarboxylates like BG1-Indo-1 and BG2-Indo-1 cannot penetrate cellular membranes, and their use as intracellular indicators is therefore restricted to the cytosol and the nucleus after invasive procedures such as microinjections. Typically, the modification of carboxylic moieties to acetoxymethyl (AM) esters

Scheme 1. Synthesis of BG1-Indo-1 (4) and BG2-Indo-1 (7)

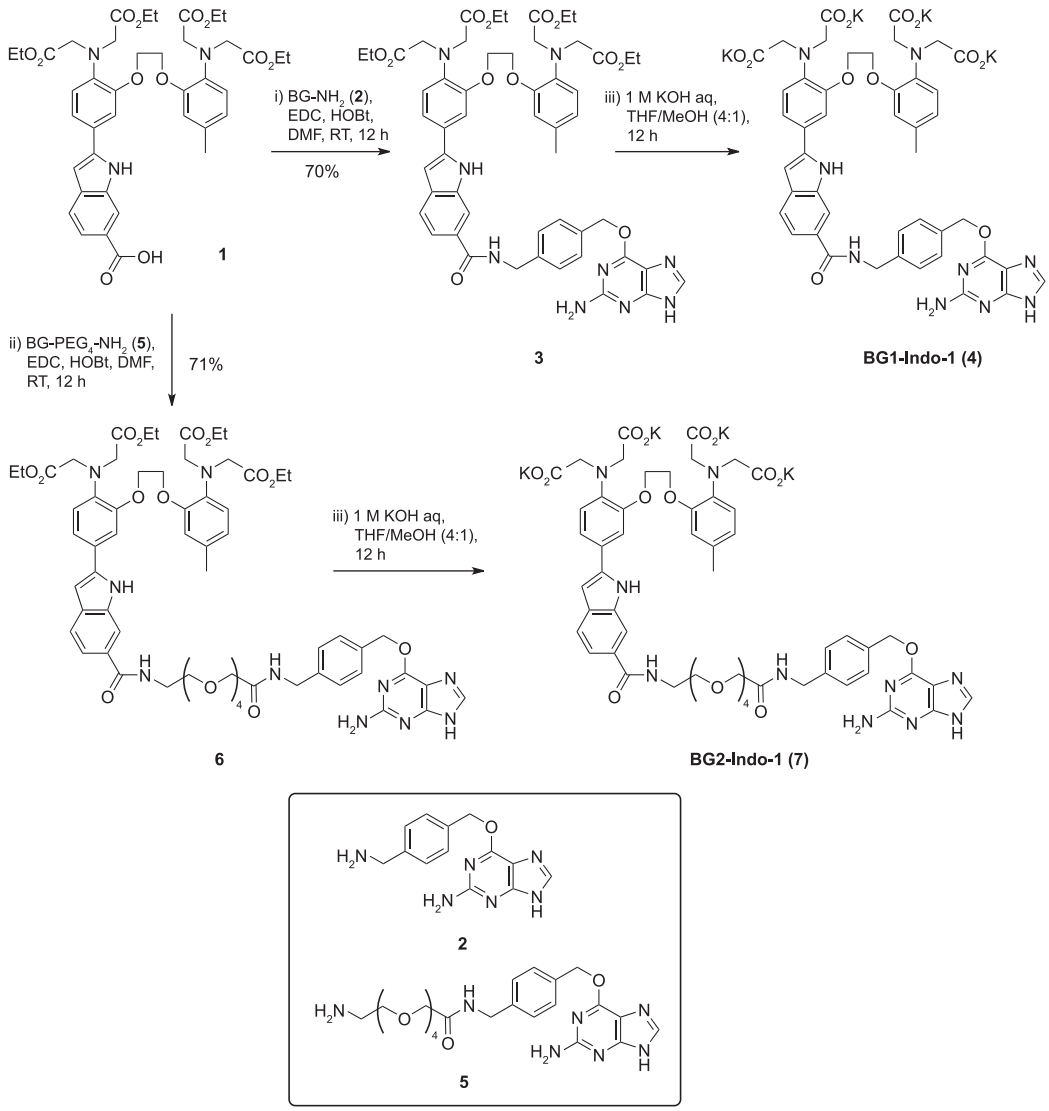

results in compounds that are membrane-permeant; once inside the cells the ester groups can be hydrolyzed by nonspecific intracellular esterases (*24*). We therefore sought to convert the two substrates into the corresponding AM ester derivatives. All attempts to directly obtain the AM esters by alkylation of BG1-Indo-1 and BG2-Indo-1 with bromomethylacetate failed. A complex mixture of products was obtained in both cases, preventing the isolation of the desired product. We therefore decided to generate an AM ester derivative of Indo-1 first and then couple it to BG *via* so-called click chemistry (*25*) (Scheme 2). Toward this end, **1** was coupled to 3-azidopropan-1-amine, and the resulting tetraethyl ester azide **8** was hydrolyzed and transformed to its corresponding acetoxymethylester **11**, which was then coupled to BG derivative **9** *via* copper (I)-catalyzed click chemistry to furnish BG3-Indo-1/AM. For the *in vitro* characterization of hydrolyzed BG3-Indo-1/AM, BG3-

SCHEME 2. Synthesis of BG3-Indo-1 (10) and BG3-Indo-1/AM (12)

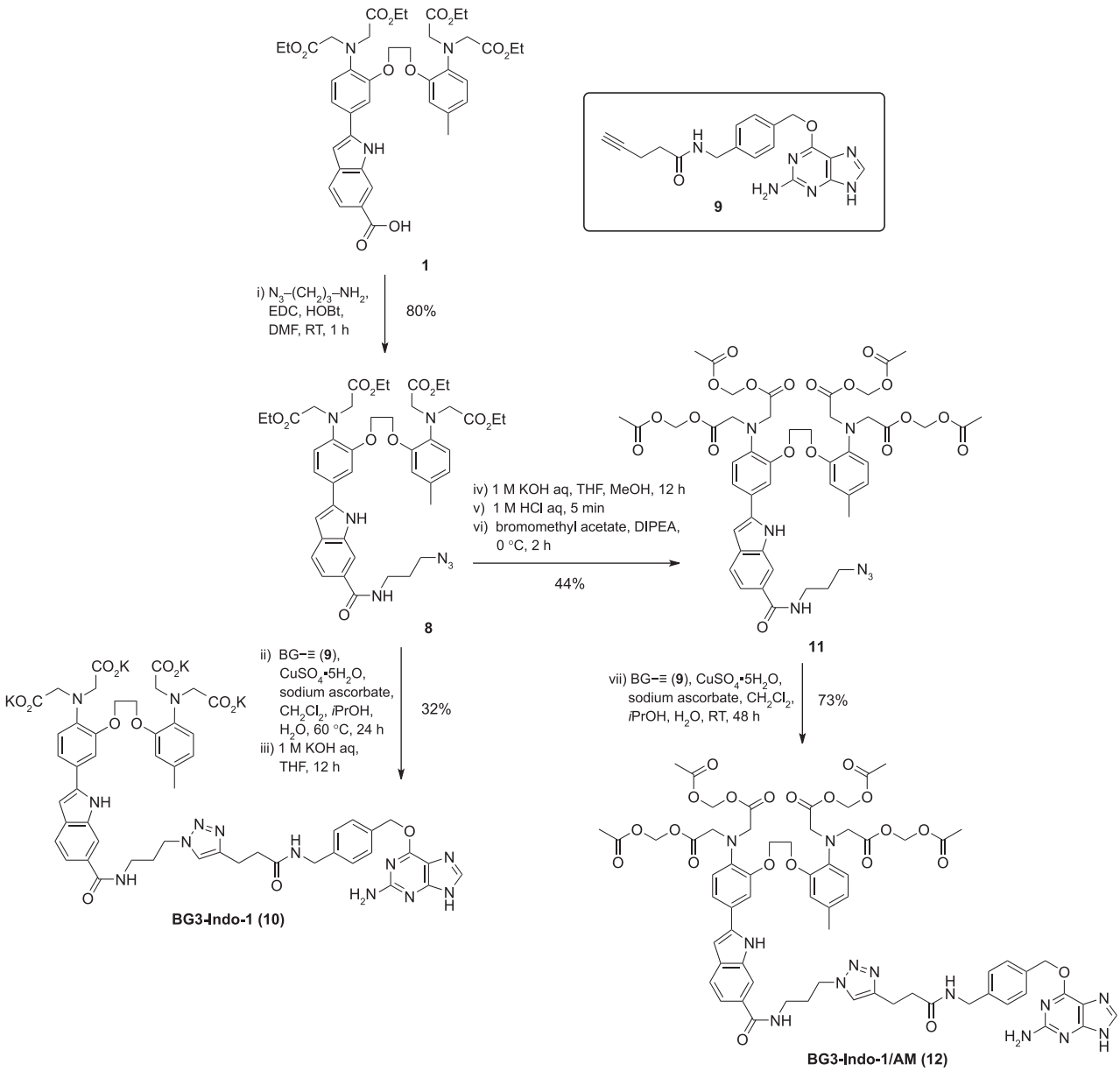

Indo-1 was synthesized *via* **8** by click chemistry followed by alkaline hydrolysis (Scheme 2).

Characterization of Indo-1 Derivatives and Their SNAP-tag Conjugates. All three BG-Indo-1 derivatives readily reacted with SNAP-tag *in vitro*. In a kinetic competition assay with BG-fluorescein (BGFL) (*26*), the observed second-order rate constants for the reaction of the Indo-1 derivatives with SNAP-tag were determined to be $(4 \pm 0.6) \times 10^4$ M^{-1} s^{-1} for BG1-Indo-1, $(9 \pm 7) \times 10^3$ M^{-1} s^{-1} for BG2-Indo-1, and $(1.4 \pm 0.2) \times 10^4$

TABLE 1. *In vitro* calibration of SNAP Indo-1 BG conjugates

		UV–vis absorption maxima [nm]		Fluorescence emission maxima [nm]		Relative quantum yield		
Dye[a]	K_D [nM]	Free anion	Ca^{2+}-bound	Free anion	Ca^{2+}-bound	Free anion	Ca^{2+}-bound	Ratio quotient[b]
SNAP + Indo-1	510 ± 270	347	331	467	419	0.37	0.30	25.2
SNAP-1-Indo-1	570 ± 170	356	340	467	419	0.49	0.38	15.8
SNAP-2-Indo-1	350 ± 90	353	338	468	421	0.26	0.27	9.3
SNAP-3-Indo-1	290 ± 80	352	338	469	420	0.42	0.36	9.5
Indo-1	270 ± 50	347	331	469	418	0.38[c]	0.56[c]	24.0
BG1-Indo-1	370 ± 180	354	334	526	428	0.06	0.14	n.d.[d]
BG2-Indo-1	180 ± 60	356	338	510	424	0.11	0.20	n.d.[d]
BG3-Indo-1	180 ± 60	358	341	508	422	0.22	0.29	n.d.[d]

[a]SNAP-1-Indo-1, SNAP-2-Indo-1 and SNAP-3-Indo-1 are the conjugates resulting from the reaction of SNAP with BG1-Indo-1, BG2-Indo-1 and BG3-Indo-1, respectively. [b]The ratio quotient is obtained by dividing the fluorescene emissions ratio 405 nm/485 nm of the calcium-bound species by that of the calcium-free species. [c]Taken from (*16*) [d]Because of the shifted emission maxima of the BG-Indo-1 derivatives, the ratio quotient at 405 nm/485 nm was not determined.

M^{-1} s^{-1} for BG3-Indo-1. At a BG-Indo-1 concentration of 1 μM and an excess of substrate over protein, labeling thus reaches 50% completion after about 1 min.

The three derivatives BG1-Indo-1, BG2-Indo-1, and BG3-Indo1 were then reacted with an excess of SNAP-tag and the resulting conjugates SNAP-1-Indo-1, SNAP-2-Indo-1, and SNAP-3-Indo-1 were characterized by UV–vis absorption and fluorescence spectroscopy. The absorption maxima of the SNAP-Indo-1 conjugates lie at 352–356 nm in the calcium-free anion form and at 338–340 nm in the calcium-bound form and are thus red-shifted by 5–9 and 7–9 nm, respectively, in comparison to Indo-1 (Table 1). Upon excitation at 350 nm, the SNAP-Indo-1 conjugates show fluorescence emission maxima for the calcium-free and the calcium-bound species very similar to those of Indo-1 (Table 1, Figure 2). Furthermore, the relative fluorescence quantum yields are comparable to those of Indo-1 (Table 1). In contrast, all BG-Indo-1 derivatives exhibit less fluorescence than the corresponding SNAP-Indo-1 conjugates and also significantly shifted emission spectra (Table 1). The reduced fluorescence is probably due to intramolecular quenching by the benzylguanine moiety. The effect is most pronounced for the derivative with the shortest linker, BG1-Indo-1, which displays a >4-fold increase of the fluorescence intensity upon reaction with SNAP (Figure 2, Table 1). This feature of the probes should be advantageous for measurements in cells as it reduces the background fluorescence from unreacted indicator. Possible explanations for the observed quenching in BG1-Indo-1 might be intramolecular stacking of the BG and Indo-1 moieties or photoinduced electron transfer from BG to Indo-1.

In conventional use calcium concentrations are measured with Indo-1 by dividing its fluorescence emission near 405 nm by the emission near 485 nm. The quotient of the ratios of the calcium-bound species (R_{max}) and the calcium-free species (R_{min}) defines the *DR* of these dyes. We determined the apparent Ca^{2+} dissociation constant K_D for the different SNAP-Indo-1 conjugates *via* their fluorescence emissions. K_D values ranged from 290 nM for SNAP-3-Indo-1 to 570 nM for SNAP-1-Indo-1 (Table 1). The presence of protein is known to cause variations in K_D of synthetic calcium indicators, typically an increase (*27, 28*). The *DR* of the SNAP-Indo-1 conjugates is lower than that of Indo-1 (Table 1 and in-cell measurements below). The decreased *DR* results from broader fluorescence emission spectra of the SNAP-Indo-1 conjugates. Effects of the presence of protein on Indo-1 fluorescence are well-known (*29*); the broader emission spectra and resulting smaller *DR* of the dyes could be due to their conjugation to a protein and the modification of the fluorophore structure.

Targeted SNAP-tag Is Expressed Specifically in Nuclei of Mouse Muscle Fibers. In muscle, cytosolic $[Ca^{2+}]$ ($[Ca^{2+}]_c$) increases by ≥2 orders of magnitude to signal contractile activation in the process called excitation-contraction coupling (*30*). This was the first messenger role demonstrated for Ca^{2+} (*31*) and is still thought to involve the largest change of concentration and fastest movements of the ion inside cells. For first proof-of-principle experiments in cells, we decided to localize the Indo-1 indicators in the nuclei of muscle cells of adult mice. Muscle fibers are large cells, with many pancake-shaped "myonuclei" normally located at the cell surface, just below the plasma membrane. Upon changes in $[Ca^{2+}]_c$, the $[Ca^{2+}]$ in the nucleoplasm equilibrates by diffusion (*32*). We chose the nucleus for this demonstration for multiple reasons, including (i) the possibility of highly specific targeting of SNAP-tag *via* the nuclear localization signal (NLS) sequence (*21*), (ii) the current interest in nuclear Ca^{2+} as a controller of transcription with signals encoded in the pattern of its concentration changes (*32*), (iii) the ease of identification of the targeted organelle, and (iv) the availability of simple procedures to change $[Ca^{2+}]_n$. Furthermore, the availability of gene transfer techniques permits to in-

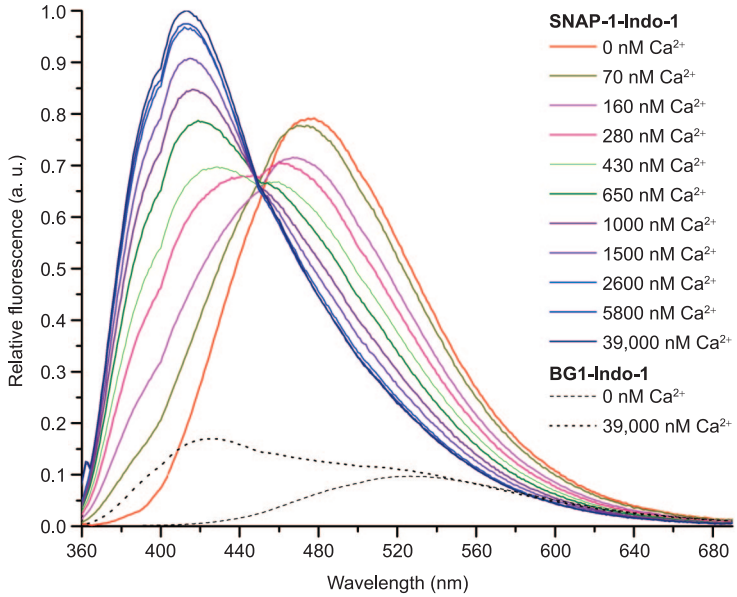

Figure 2. Fluorescence spectra of SNAP-1-Indo-1 (200 nM) and BG1-Indo-1 at varying calcium concentrations with excitation at 350 nm. Both the wavelength shift upon calcium binding and the fluorescence emission intensity increase after the reaction of BG1-Indo-1 with SNAP-tag are clearly visible.

duce expression of virtually any protein at high densities in these cells (*33*) (*34*).

First, we validated the expression of a functional SNAP-tag fusion inside myonuclei in cells of the paw muscle FDB, as a specific labeling of SNAP-tag fusion proteins in cells of an adult, living animal has previously not been demonstrated. The hind paws of 2-month-old mice were injected with a plasmid vector coding for SNAP-NLS and cells were transfected by electroporation. Four to five days after injection, individual cells were isolated, separated by enzymatic digestion, stained by brief exposure to the cell-permeant substrate BG-diacetylfluorescein (BG-DAF), and examined by confocal imaging of fluorescence. The nonfluorescent and membrane-permeant BG-DAF is hydrolyzed to the corresponding fluorescein derivative in the cell (*21*). Typical images are shown in Figure 3. Panel a is an image of a fiber obtained after labeling with BG-DAF, at a low intensity of excitation. Under these conditions only nuclei are visible, demonstrating specific labeling of nuclear localized SNAP-tag. Panel b is an image at a 5 times greater excitation intensity, which demonstrates some fluorescence outside nuclei. Similar background fluorescence is observed in the fluorescence image of a fiber from nontransfected muscle after a similar incubation with BG-DAF (Figure 3, panel c). This implies that the extranuclear fluorescence is not due to mistargeted SNAP-NLS; it could be due to cellular autofluorescence or excess BG-DAF that did not react with SNAP-NLS. To separate these contributions we measured the fluorescence of a fiber expressing SNAP-NLS but not exposed to BG-DAF, acquired at the same excitation intensity and gain. The image is displayed in Figure 3, panel d, using a color scale expanded 7-fold. Thus the cellular autofluorescence in Panel D is about 15% of the total background fluorescence in Panel C. In conclusion, the SNAP-NLS fusion expresses at high density in the nuclei of mouse muscle fibers, where it can be specifically labeled with BG derivatives.

Localized Indo-1 Senses Calcium in the Cell Nucleus. To localize Indo-1 in myonuclei, cells treated as described in the previous section, with plasma membrane intact, were incubated with BG3-Indo-1/AM for 210 min at RT. After washing and allowing 30−60 min for hydrolysis of the AM esters, the fluorescence was imaged by confocal microscopy. Two images of fluorescence, F_1 and F_2, were obtained simultaneously at two excitation wavelengths and two emission ranges pre-

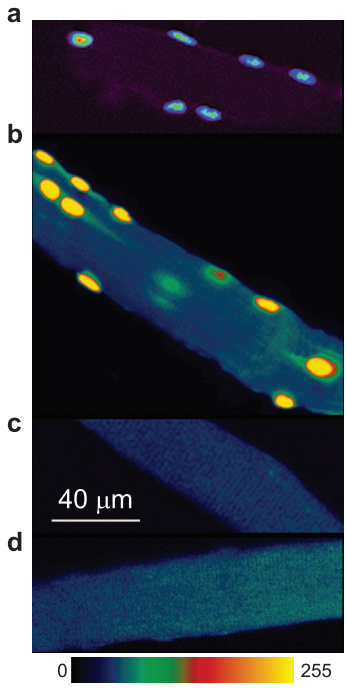

Figure 3. Localization of SNAP-tag in nuclei of muscle fibers. a) Confocal image of fluorescence of a cell isolated from the FDB muscle of a mouse expressing SNAP-NLS. The cell had been briefly exposed to BG-DAF (1 μM, 3−4 min). Image obtained at low excitation intensity (power of Ar laser at 488 nm was set at 3% of maximum). Fluorescence is emitted by fluorescein set free from hydrolysis of diacetylfluorescein (DAF) and originates largely at nuclei. b) Image of a different segment of the same fiber at greater excitation intensity (15%), to show staining outside nuclei, presumably by BG-DAF not bound to SNAP-NLS or cellular autofluorescence. c) Fluorescence of a fiber not expressing SNAP-NLS but exposed to BG-DAF; image acquired at the same excitation intensity as in panel b. Gain-determining photomultiplier voltage was the same in all cases. d) Fluorescence of a fiber expressing SNAP-NLS but not exposed to BG-DAF, acquired at same excitation intensity and gain but displayed in a color scale expanded 7-fold (*i.e.*, the covered range is 0−36 units in this case). This image indicates that cellular autofluorescence level in panel d is ~15% of the background fluorescence in panel c.

scribed by the SEER method (*17*), and the ratio $R = F_1/F_2$ was determined. A representative example is shown in Figure 4, panels a−c. Again, the staining is highly specific to nuclei. Compared to staining with BG-DAF, however, there is somewhat greater fluorescence outside nuclei, especially F_1 (Figure 4, panel a), which is shown at a 4× greater intensity than F_2 in order to demonstrate the nonspecific fluorescence. The extranuclear fluorescence is presumably due to both unreacted BG3-Indo-1 and to cellular autofluorescence, which is preferentially excited and emitted at lower wavelengths. In the three nuclei that were in focus in images a and b, the average value of the ratio $R = F_1/F_2$ was low, 0.48 (standard deviation 0.056) (Figure 4, panel c). The nominal $[Ca^{2+}]_n$, calculated using eq 1 (Methods) and calibration parameters obtained as described below, was 109 nM. The average R for nine intact cells (an equally weighted average of averages over all stained nuclei in individual cells) was 0.37 (standard deviation 0.12), which corresponds to a $[Ca^{2+}]_n$ of 37 nM. This value is consistent with the low cytosolic and nuclear $[Ca^{2+}]$ that prevails in a resting muscle cell (*32*).

To demonstrate the response of the sensor to changes in $[Ca^{2+}]_n$ and to calibrate it, we applied buffered solutions of different $[Ca^{2+}]$ to cells with the plasma membrane permeabilized (by brief exposure to a low concentration of saponin; see Methods) and incubated with BG3-Indo-1/AM for 6−9 min in a solution that was nominally Ca^{2+}-free. An experiment is illustrated in Figure 5, panels a and b of which are images of F_1 and F_2 for a representative cell immediately after permeabilization, incubation, and exposure to a bathing solution of 100 nM $[Ca^{2+}]$. Four nuclei are clearly visible. The cell was then successively exposed to additional solutions with increasing $[Ca^{2+}]$. Figure 5, panels c−e are images of R (restricted to areas of high staining as in Figure 4) upon exposure to $[Ca^{2+}]$ of 100 nM (c), 1 μM (d), and 10 μM (e). The high $[Ca^{2+}]$ solutions caused some movement of the cell and loss of focus for two nuclei. This was repeated in three experiments. The graph in Figure 5, panel f plots the averaged R values against the applied $[Ca^{2+}]$ (points *c*, *d*, *e*). The single point *g* plots a reading obtained immediately after membrane permeabilization in a solution with nominally 0 $[Ca^{2+}]$. The continuous curve in red represents the best fit to all points by a conventional equation relating SEER ratio and concentration (eq 2, Methods) with three free parameters whose best fit values are given in the legend. The curve in black plots an alternative fit obtained by forcing R_{min} and R_{max} to be equal to, respectively, the values obtained at 0 and 10 μM (a change without major consequences for the fit). The open circle plots the average R in intact cells at its intersection with the red curve, yielding a $[Ca^{2+}]_n$ of 37 nM.

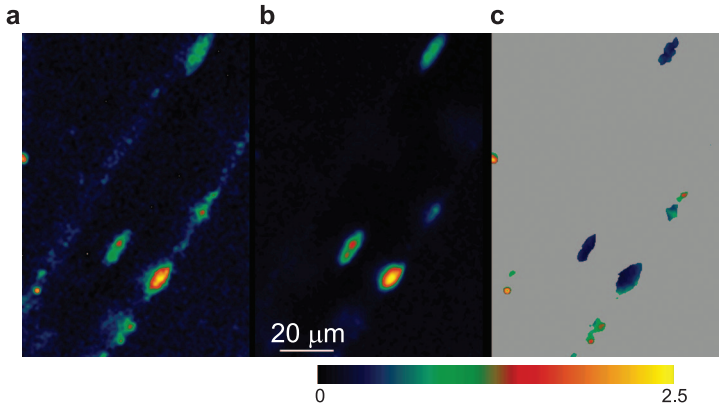

Figure 4. Localization of SNAP-3-Indo-1 to myonuclei. a,b) SEER image pair (F_1 and F_2) of a muscle cell expressing nuclear-targeted SNAP-tag, loaded with BG3-Indo-1/AM. The image in panel a is represented at 4× normal intensity to show that some extranuclear staining is present. c) $R = F_1/F_2$ restricted to regions where the sensor concentration was greater than a threshold. Three nuclei are well defined in both images, and the value of R averaged over these nuclei corresponds to a $[Ca^{2+}]_n = 109$ nM. The color bar calibrates the R image in panel c.

Conclusions. The measurement of fluctuations of $[Ca^{2+}]$ in defined locations in the cell and with adequate temporal resolution is a challenge in cell biology. Here we have introduced derivatives of the Ca^{2+} sensor Indo-1 that can be specifically coupled to SNAP-tag fusion proteins in living cells, resulting in their precise localization through the localization of the corresponding SNAP-tag fusion. In the following we will briefly summarize the properties, applications, and further developments of such hybrid indicators.

By synthesizing BG-Indo-1 derivatives with different linker lengths, we were able to show that the length of the linker does not significantly affect the spectroscopic properties of the corresponding SNAP-tag conjugates. More importantly, we found that the coupling of BG to Indo-1 led to considerable quenching of the fluorescence of Indo-1 and that the quenching disappeared upon reaction of the derivatives with SNAP-tag fusions. The effect was most pronounced for the derivative with the shortest linker, BG1-Indo-1, where the reaction with SNAP-tag led to a >4-fold increase in fluorescence. This is an attractive feature of the Indo-1 derivatives and in particular of BG1-Indo-1 as it reduces background fluorescence from unreacted dye and should therefore facilitate experiments in living cells. Initial attempts to convert BG1-Indo-1 in the corresponding AM ester were unsuccessful; however the related BG3-Indo-1/AM could be obtained *via* an alternative route.

By incubating muscle cells expressing SNAP-NLS with BG3-Indo-1/AM, we were then able to show (i) that BG3-Indo-1/AM is membrane-permeant, (ii) that it permits a targeting of Indo-1 to the nucleus of living cells and (iii) that the resulting SNAP-3-Indo-1 indicators can be used for sensing local $[Ca^{2+}]$ by SEER. For a preliminary calibration of nuclear localized SNAP-3-Indo-1, permeabilized cells were incubated with different $[Ca^{2+}]$. On the basis of these measurements, we determined $[Ca^{2+}]_n$ in isolated resting muscle cells of adult mice to be around 50 nM, a value that is in agreement with previous measurements (*32*). The measured K_D of SNAP-3-Indo-1 for Ca^{2+} in the nuclei of muscle cells was 228 nM (Figure 5, panel f) and thus comparable to the K_D value of 290 nM measured for SNAP-3-Indo-1 in a cuvette (Table 1). In general, the specific and covalent coupling of a synthetic sensor to a protein should make its microenvironment *in vitro* and in living cells more comparable and therefore its properties more predictable. Furthermore, the calibration of a fluorescent sensor such as Indo-1 usually requires permeabilization of the cell to expose the sensor to defined concentrations of analyte. The irreversible coupling of Indo-1 to a localized protein decreases the risk of translocation or leakage of the dye during and after permeabilization that would interfere with calibration measurements. Another attractive feature of the covalent coupling of Indo-1 to SNAP-tag is that it should prevent leakage of Indo-1 out of intact cells or organelles during long-term measurements, a

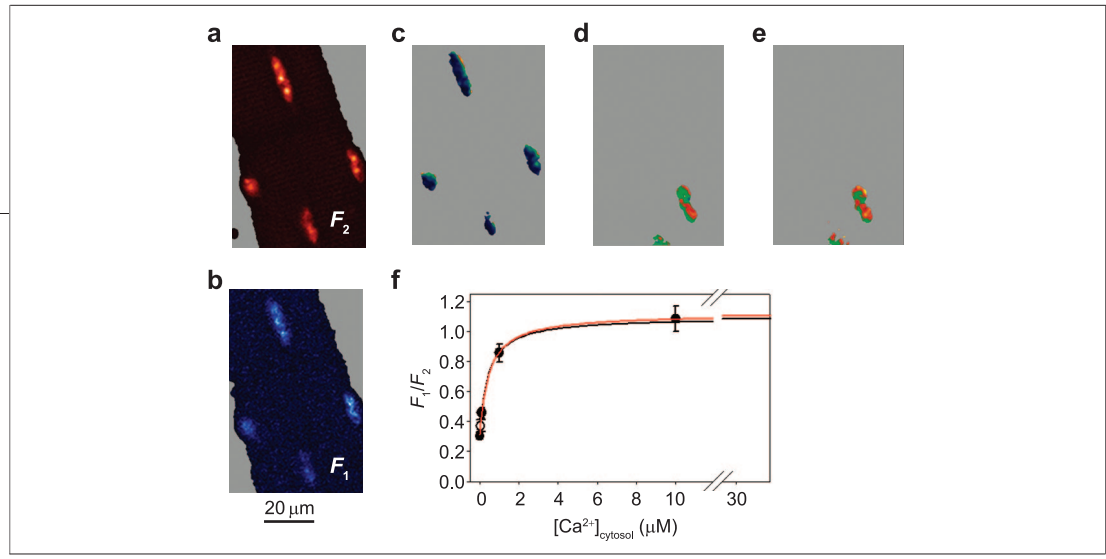

Figure 5. Calibration of SNAP-3-Indo-1 in myonuclei. a,b) SEER image pair in a membrane-permeabilized cell expressing SNAP-NLS, incubated with BG3-Indo-1/AM and then exposed to a 100 nM Ca^{2+} internal solution. c−e) $R = F_1/F_2$ (restricted to regions where the sensor concentration was greater than a threshold; same color table as in Figure 4, panel c) for cell in panels a and b after exposure to internal solutions with [Ca^{2+}] of 100 nM (c), 1 μM (d) or 100 μM (e). Incubation with 1 μM or higher [Ca^{2+}] led to cell movement, and only 2 nuclei remained in focus. f) Plot of averaged R *vs* [Ca^{2+}] in internal solution after permeabilization (bars span ± SEM in three cells, point at 0 nM represents a single measurement). The curve in red plots the best fit by eq 2 (Methods) with 3 free parameters, of values $R_{min} = 0.305$, $R_{max} = 1.17$, and $\gamma K_D = 458$ nM ($K_D = 228$ nM). The curve in black represents the constrained fit with $R_{min} = 0.301$ (the reading at 0 [Ca^{2+}]) and $R_{max} = 1.09$ (the average reading at 10 μM). In this case $\gamma K_D = 412$ nM. The open circle plots the average value of R ± SEM in nine intact cells at the abscissa calculated with the unconstrained 3-parameter fit, yielding a $[Ca^{2+}]_n$ of 37 nM.

known problem with synthetic Ca^{2+} indicators (*35, 36*). It should also be noted that the loading of intact cells with BG3-Indo-1/AM requires some 3 h at RT, which is longer than what is observed for simple dyes such as mag-indo-1/AM. In a comparison of loading rates of 13 dyes into the myoplasm of frog muscle, it was found that the rate was inversely associated with the molecular weight of the indicator (*37*). The relatively slow uptake of BG3-Indo-1/AM thus might be due to its high molecular weight.

A shortcoming of the SNAP-Indo-1 conjugates introduced here is the reduced *DR* of the compounds relative to Indo-1. Our preliminary calibration of Figure 5 for SNAP-3-Indo-1 yielded a R_{max} and R_{min} consistent with a *DR* of ~4, while calibration of Indo-1 in primary myotubes using the same experimental setup yielded a *DR* of 7.8 (*38*). Ideally, future versions of BG-Indo-1 will lead to sensors with an increased *DR* as well as a further increased quenching of the fluorescence of Indo-1 prior to the reaction with SNAP-tag. In addition, the availability of BG-dye derivatives with different K_D's for Ca^{2+} should significantly extend the range of possible applications of the approach. Our current work is focusing on these opportunities.

In summary, we have introduced derivatives of the fluorescent Ca^{2+} sensor Indo-1 that can be localized in living cells through the specific reaction with SNAP-tag fusion proteins. The resulting hybrid indicators combine the spatial specificity of biosensors with the fast kinetics and high dynamic range of small synthetic indicators. In addition to the sensing of organellar or local [Ca^{2+}], the covalent and irreversible coupling of Indo-1 to SNAP-tag fusion proteins should also facilitate the calibration of the sensor and long-term measurements in living cells as it prevents translocation and leakage of the indicator. These features should make the approach a valuable addition to the existing methods to sense [Ca^{2+}] in cells.

METHODS

Organic Synthesis. Detailed protocols on the syntheses of the reported Indo-1 derivatives are described in Supporting Information.

In Vitro Fluorescent Measurements. SNAP-tag used in this work has been described previously (*22*) and is a truncated version of human wild-type AGT (182 amino acids) that carries the following mutations: K32I, L33F, C62A, Q115S, Q116H, K125A, A127T, R128A, G131K, G132T, M134L, R135S, C150Q, S151G, S152D, G153L, A154D, N157G, and S159E. SNAP-tag was expressed in *Escherichia coli* BL21 (DE3) with the expression plasmid pET-15b as a hexahistidine fusion protein and purified by metal chelate chromatography (*39*). The kinetics of the reaction of Indo-1 BG derivatives with SNAP-tag were determined in a competition assay with BGFL as previously described (*26*). In short, SNAP-tag (0.25 μM) was incubated with BGFL (1 μM) and varying concentrations of the BG-Indo-1 derivative (0.33, 1, or 3 μM) in PBS. The amount of SNAP-tag that reacted with BGFL was determined by fluorescence scanning after SDS-PAGE (Pharos FX Molecular Imager, Bio-Rad).

Fluorescence emission spectra were recorded on a SPEX Fluorolog-3 spectrofluorometer (Horiba Jobin Yvon) in a 10 mm × 4 mm quartz semimicro cell, upon excitation at 350 nm. Excitation and emission bandwidths were set to 7 and 10 nm, re-

spectively. The fluorescence spectrum (recorded from 360 to 700 nm) was obtained choosing a step size of 1 nm and an integration time of 1.0 s step^{-1}.

Additional fluorescence spectra were measured on a Molecular Devices FlexStation. Solutions of 1 μM concentration of Indo-1 derivative were used, where applicable SNAP-tag was added at 2 μM concentration. Calcium concentrations were controlled by using the Molecular Probes Calcium buffer kit with 30 mM MOPS/KOH, pH = 7.2, 100 mM KCl and 10 mM EGTA or 10 mM CaEGTA, respectively. Fluorescence intensities were measured in 96-well plates containing 200 μL of solution in each well, using either clear-bottom micro plates (Greiner) in the bottom read mode or black micro test assay plates (Becton Dickinson) in the top read mode. The spectra were recorded at a 9 nm bandwidth. Spectra were recorded at step-size and then averaged over 9 nm. Ratios were calculated at 405 and 485 nm ($R = F_{405\ nm}/F_{485\ nm}$) or at other wavelengths where indicated. Ratio quotients or dynamic ranges, respectively, were calculated by dividing the calcium complex intensity ratio by the appropriate value of the free anion form ratio: $RQ = R_{Ca^{2+}\ complex}/R_{free\ anion} = R_{max}/R_{min}$ at 405 and 485 nm. Relative quantum yields were calculated by comparing the integrated fluorescence intensity of the Indo-1 derivatives with Indo-1 (*16*) over the range 385−650 nm and dividing by their respective absorbance at the excitation wavelength (350 nm). Absorbance spectra of samples containing 10 μM Indo-1 derivatives in a microcuvette were recorded with a Perkin-Elmer Lambda 10 UV−vis spectrometer. Apparent calcium binding constants were calculated from the fluorescence spectra using plots of log $[(R - R_{min})/(R_{max} - R)]\cdot[(F_{free\ anion,485\ nm})/(F_{Ca^{2+}\ complex,485\ nm})]$ against log $[Ca^{2+}{}_{free}]$ as previously described (*16*).

Transfection of FDB Muscle by Electroporation in Adult Mice. Protocols using mice were approved by the IACUC of Rush University. The ventral side of both hind paws of 2-month-old mice anaesthetized by isoflurane was cleaned with 75% ethanol. Then, 10 μL of 2 mg mL^{-1} hyaluronidase dissolved in sterile saline was injected into the center of each paw through a 29-gauge needle. One hour later, 10 μL of solution (20 μg DNA in sterile saline) was injected subcutaneously. The plasmid used, containing three consecutive simian virus 40 (SV40) large T antigen nuclear localization sequences (NLS) fused at the C terminus of SNAP-tag, was named pCMV-SNAP-NLS$_3$. Ten minutes later, two electrodes (gold-plated stainless steel acupuncture needles) were placed subcutaneously at the starting lines of paw and toes, separated ~9 mm. Twenty pulses of 100 V cm^{-1} and 20 ms were applied at 1 Hz (using an ECM 830 Electro Square Porator, BTX). Six to 10 days later, the animal was sacrificed by CO_2 inhalation, and FDB muscles were removed for imaging or functional studies.

Isolation of Single Cells and Generation of Hybrid Indicator in Cells. The FDB was surgically removed and placed in a 0 Ca^{2+} Tyrode's solution containing 0.2% collagenase (C0130, Sigma) for 40−55 min (depending on animal weight and collagenase lot variability) at 37 °C. Single fibers were dissociated by gently passing the digested muscle for a few times through Pasteur pipettes. The fibers were kept at 4 °C in Tyrode's solution. Aliquots of this suspension of intact cells were loaded in Tyrode's solution plus 5 μM BG3-Indo-1/AM and 1% pluronic for 3−4 h at RT. Membrane permeabilization was produced by exposure for 2−3 min to a nominally Ca^{2+}-free internal solution plus 0.002% saponin (*38, 40*). For visualization of the expressed SNAP-NLS, the suspension of intact cells, placed in the observation chamber on the microscope stage, was exposed to Tyrode's solution containing 1 μM BG-DAF for 3−4 min. All imaging reported here was carried out at RT (20−21 °C).

Microscopy and Image Processing. The optical implementation of SEER consisted in the simultaneous acquisition of two confocal images, produced by alternating line by line ("line-interleaving") two excitation lights and two fluorescence emission ranges. *xy* scans of 512 × 512 pixels at 0.23 or 0.13 μm distance were obtained line-interleaved in the range 390−440 nm with 351 nm excitation (F_1, Figure 5, panel b) and in the range 465−535 nm with 364 nm excitation (F_2, Figure 5, panel a). Scanning was done with the Leica TCS SP2 confocal system (Leica Microsystems, Exton, PA), which defines detection bands spectrally and switches excitation *via* acousto-optical tunable filters and beam splitters.

For calculation of $[Ca^{2+}]_n$, ratio values ($R(x,y) = F_1(x,y)/F_2(x,y)$) were averaged over all pixels within every nucleus in the image. Individual nuclei were defined as areas of the image where the local bioindicator concentration (calculated by a linear combination of values F_1 and F_2 that is invariant upon changes in $[Ca^{2+}]$ (*17*)) exceeds a threshold set empirically. These ratios were assumed to correspond monotonically to $[Ca^{2+}]$ according to

$$[Ca^{2+}] = \gamma K_D \frac{R - R_{min}}{R_{max} - R} \quad (1)$$

where K_D is the dissociation constant of the indicator and γ is the ratio of F_2 in free and Ca^{2+}-complexed sensor (*17*). Calibration of the relationship was carried out by fitting $R([Ca^{2+}])$ data with the function derived solving eq 1 for *R*, and free parameters R_{max}, R_{min}, and γK_D

$$R = \frac{R_{max}[Ca^{2+}] + R_{min}\gamma K_D}{[Ca^{2+}] + \gamma K_D} \quad (2)$$

The best fit parameter values were $R_{max} = 1.17$, $R_{min} = 0.305$,and $\gamma K_D = 458$ nM; γ was 2.01.

The composition of the buffer used for calibrations in permeabilized cells was as described previously (*38*). Briefly, it was based on potassium glutamate, with added EGTA (1 mM), ATP (5 mM), phosphocreatine (5 mM), dextran (8%), glucose (5 mM), trizma, $MgCl_2$ for a final free $[Mg^{2+}]$ of 2 mM, and $CaCl_2$ of 0, 0.351, 0.847, or 1.01 mM for a final free $[Ca^{2+}]$ of 0, 0.1, 1, or 10 μM. The solutions were titrated with KOH for a pH of 7.2, and the osmolarity was set to 300 mOsm. The composition of Tyrode's solution was as described previously (*38*).

Acknowledgment: We thank Dr. Simone Schmitt for providing hexahistine-tagged SNAP-tag and Drs. Ruud Hovius and Marlon Hinner for discussions. This work was supported by grants from the Swiss National Science Foundation and Human Frontier Science Program (to K.J.) and grants AR032808 and AR049184 from the National Institute of Arthritis and Musculoskeletal and Skin Diseases, National Institutes of Health, USA (to E.R.). M.B. holds a Marie Curie Intra-European fellowship (contract number MEIF-CT-2007-038746). M.Z. was supported by a grant-in-aid from the Muscular Dystrophy Association of America to Dr. Jingsong Zhou (Rush University), to whom we are grateful for her support.

Supporting Information Available: This material is available free of charge *via* the Internet at http://pubs.acs.org.

REFERENCES

1. Clapham, D. E. (2007) Calcium signaling, *Cell 131*, 1047–1058.
2. Csordas, G., Thomas, A. P., and Hajnoczky, G. (1999) Quasi-synaptic calcium signal transmission between endoplasmic reticulum and mitochondria, *Embo J. 18*, 96–108.
3. Niggli, E., and Shirokova, N. (2007) A guide to sparkology: the taxonomy of elementary cellular Ca^{2+} signaling events, *Cell Calcium 42*, 379–387.

4. Miyawaki, A., Llopis, J., Heim, R., McCaffery, J. M., Adams, J. A., Ikura, M., and Tsien, R. Y. (1997) Fluorescent indicators for Ca^{2+} based on green fluorescent proteins and calmodulin, *Nature 388*, 882–887.
5. Romoser, V. A., Hinkle, P. M., and Persechini, A. (1997) Detection in living cells of Ca^{2+}-dependent changes in the fluorescence emission of an indicator composed of two green fluorescent protein variants linked by a calmodulin-binding sequence. A new class of fluorescent indicators, *J. Biol. Chem. 272*, 13270–13274.
6. Baird, G. S., Zacharias, D. A., and Tsien, R. Y. (1999) Circular permutation and receptor insertion within green fluorescent proteins, *Proc. Natl. Acad. Sci. U.S.A. 96*, 11241–11246.
7. Nakai, J., Ohkura, M., and Imoto, K. (2001) A high signal-to-noise Ca^{2+} probe composed of a single green fluorescent protein, *Nat. Biotechnol. 19*, 137–141.
8. Mank, M., and Griesbeck, O. (2008) Genetically encoded calcium indicators, *Chem. Rev. 108*, 1550–1564.
9. Palmer, A. E., and Tsien, R. Y. (2006) Measuring calcium signaling using genetically targetable fluorescent indicators, *Nat. Protoc. 1*, 1057–1065.
10. Garaschuk, O., Griesbeck, O., and Konnerth, A. (2007) Troponin C-based biosensors: a new family of genetically encoded indicators for *in vivo* calcium imaging in the nervous system, *Cell Calcium 42*, 351–361.
11. Rutter, G. A., Burnett, P., Rizzuto, R., Brini, M., Murgia, M., Pozzan, T., Tavare, J. M., and Denton, R. M. (1996) Subcellular imaging of intramitochondrial Ca^{2+} with recombinant targeted aequorin: significance for the regulation of pyruvate dehydrogenase activity, *Proc. Natl. Acad. Sci. U.S.A. 93*, 5489–5494.
12. Allbritton, N. L., Oancea, E., Kuhn, M. A., and Meyer, T. (1994) Source of nuclear calcium signals, *Proc. Natl. Acad. Sci. U.S.A. 91*, 12458–12462.
13. Etter, E. F., Kuhn, M. A., and Fay, F. S. (1994) Detection of changes in near-membrane Ca^{2+} concentration using a novel membrane-associated Ca^{2+} indicator, *J. Biol. Chem. 269*, 10141–10149.
14. Marks, K. M., Rosinov, M., and Nolan, G. P. (2004) *In vivo* targeting of organic calcium sensors *via* genetically selected peptides, *Chem. Biol. 11*, 347–356.
15. Tour, O., Adams, S. R., Kerr, R. A., Meijer, R. M., Sejnowski, T. J., Tsien, R. W., and Tsien, R. Y. (2007) Calcium Green FlAsH as a genetically targeted small-molecule calcium indicator, *Nat. Chem. Biol. 3*, 423–431.
16. Grynkiewicz, G., Poenie, M., and Tsien, R. Y. (1985) A new generation of Ca^{2+} indicators with greatly improved fluorescence properties, *J. Biol. Chem. 260*, 3440–3450.
17. Launikonis, B. S., Zhou, J., Royer, L., Shannon, T. R., Brum, G., and Rios, E. (2005) Confocal imaging of $[Ca^{2+}]$ in cellular organelles by SEER, shifted excitation and emission ratioing of fluorescence, *J. Physiol. 567*, 523–543.
18. Jackson, A. P., Timmerman, M. P., Bagshaw, C. R., and Ashley, C. C. (1987) The kinetics of calcium binding to fura-2 and indo-1, *FEBS Lett. 216*, 35–39.
19. Sanchez-Martin, R. M., Cuttle, M., Mittoo, S., and Bradley, M. (2006) Microsphere-based real-time calcium sensing, *Angew. Chem., Int. Ed. 45*, 5472–5474.
20. Belan, P. V., Gerasimenko, O. V., Berry, D., Saftenku, E., Petersen, O. H., and Tepikin, A. V. (1996) A new technique for assessing the microscopic distribution of cellular calcium exit sites, *Pflugers Arch. 433*, 200–208.
21. Keppler, A., Gendreizig, S., Gronemeyer, T., Pick, H., Vogel, H., and Johnsson, K. (2003) A general method for the covalent labeling of fusion proteins with small molecules *in vivo*, *Nat. Biotechnol. 21*, 86–89.
22. Gronemeyer, T., Chidley, C., Juillerat, A., Heinis, C., and Johnsson, K. (2006) Directed evolution of O6-alkylguanine-DNA alkyltransferase for applications in protein labeling, *Protein Eng. Des. Sel. 19*, 309–316.
23. Keppler, A., Pick, H., Arrivoli, C., Vogel, H., and Johnsson, K. (2004) Labeling of fusion proteins with synthetic fluorophores in live cells, *Proc. Natl. Acad. Sci. U.S.A. 101*, 9955–9959.
24. Tsien, R. Y. (1981) A non-disruptive technique for loading calcium buffers and indicators into cells, *Nature 290*, 527–528.
25. Rostovtsev, V. V., Green, L. G., Fokin, V. V., and Sharpless, K. B. (2002) A stepwise huisgen cycloaddition process: copper(I)-catalyzed regioselective "ligation" of azides and terminal alkynes, *Angew. Chem., Int. Ed. 41*, 2596–2599.
26. Gautier, A., Juillerat, A., Heinis, C., Correa, I. R., Jr., Kindermann, M., Beaufils, F., and Johnsson, K. (2008) An engineered protein tag for multiprotein labeling in living cells, *Chem. Biol. 15*, 128–136.
27. Harkins, A. B., Kurebayashi, N., and Baylor, S. M. (1993) Resting myoplasmic free calcium in frog skeletal muscle fibers estimated with fluo-3, *Biophys. J. 65*, 865–881.
28. Hove-Madsen, L., and Bers, D. M. (1992) Indo-1 binding to protein in permeabilized ventricular myocytes alters its spectral and Ca binding properties, *Biophys. J. 63*, 89–97.
29. Baker, A. J., Brandes, R., Schreur, J. H., Camacho, S. A., and Weiner, M. W. (1994) Protein and acidosis alter calcium-binding and fluorescence spectra of the calcium indicator indo-1, *Biophys. J. 67*, 1646–1654.
30. Sandow, A. (1952) Excitation-contraction coupling in muscular response, *Yale J. Biol. Med. 25*, 176–201.
31. Heilbrunn, L. V., and Wiercinski, F. J. (1947) The action of various cations on muscle protoplasm, *J. Cell. Comp. Physiol. 29*, 15–32.
32. Gerasimenko, O., and Gerasimenko, J. (2004) New aspects of nuclear calcium signalling, *J. Cell. Sci. 117*, 3087–3094.
33. DiFranco, M., Neco, P., Capote, J., Meera, P., and Vergara, J. L. (2006) Quantitative evaluation of mammalian skeletal muscle as a heterologous protein expression system, *Protein Expression Purif. 47*, 281–288.
34. Pouvreau, S., Royer, L., Yi, J., Brum, G., Meissner, G., Rios, E., and Zhou, J. (2007) Ca^{2+} sparks operated by membrane depolarization require isoform 3 ryanodine receptor channels in skeletal muscle, *Proc. Natl. Acad. Sci. U.S.A. 104*, 5235–5240.
35. Roe, M. W., Lemasters, J. J., and Herman, B. (1990) Assessment of Fura-2 for measurements of cytosolic free calcium, *Cell Calcium 11*, 63–73.
36. Di Virgilio, F., Steinberg, T. H., and Silverstein, S. C. (1990) Inhibition of Fura-2 sequestration and secretion with organic anion transport blockers, *Cell Calcium 11*, 57–62.
37. Zhao, M., Hollingworth, S., and Baylor, S. M. (1997) AM-loading of fluorescent Ca^{2+} indicators into intact single fibers of frog muscle, *Biophys. J. 72*, 2736–2747.
38. Zhou, J., Yi, J., Royer, L., Launikonis, B. S., Gonzalez, A., Garcia, J., and Rios, E. (2006) A probable role of dihydropyridine receptors in repression of Ca^{2+} sparks demonstrated in cultured mammalian muscle, *Am. J. Physiol. Cell Physiol. 290*, C539–553.
39. Sielaff, I., Arnold, A., Godin, G., Tugulu, S., Klok, H. A., and Johnsson, K. (2006) Protein function microarrays based on self-immobilizing and self-labeling fusion proteins, *ChemBioChem 7*, 194–202.
40. Zhou, J., Brum, G., Gonzalez, A., Launikonis, B. S., Stern, M. D., and Rios, E. (2003) Ca^{2+} sparks and embers of mammalian muscle. Properties of the sources, *J. Gen. Physiol. 122*, 95–114.